Identification of Two Nervous System-Specific Members of the *erg* Potassium Channel Gene Family

Wenmei Shi,[1] Randy S. Wymore,[2] Hong-Sheng Wang,[2] Zongming Pan,[1] Ira S. Cohen,[1] David McKinnon,[1,2] and Jane E. Dixon[1]

[1]Departments of Neurobiology and Behavior and [2]Physiology and Biophysics, State University of New York at Stony Brook, Stony Brook, New York 11794

Two new potassium channel genes, *erg*2 and *erg*3, that are expressed in the nervous system of the rat were identified. These two genes form a small gene family with the previously described *erg*1 (HERG) gene. The *erg*2 and *erg*3 genes are expressed exclusively in the nervous system, in marked contrast to *erg*1, which is expressed in both neural and non-neural tissues. All three genes are expressed in peripheral sympathetic ganglia. The *erg*3 channel produces a current that has a large transient component at positive potentials, whereas the other two channels are slowly activating delayed rectifiers. Expression of the *erg*1 gene in the sympathetic nervous system has potential implications for the etiology of the LQT2 form of the human genetic disease long QT syndrome.

Key words: potassium channel; erg*; long QT syndrome; sympathetic neuron; gene; delayed rectifier*

A family of three related voltage-gated potassium channel genes (*eag*, *erg*, and *elk*) has been described in either *Drosophila* or mammals (Warmke et al., 1991; Ludwig et al., 1994; Warmke and Ganetzky, 1994; Titus et al., 1997; Wang et al., 1997). These channels share the six-membrane-spanning architecture of the Kv class (*Shaker*-related) of voltage-gated potassium channels but otherwise are distantly related to the Kv class channels (Warmke and Ganetzky, 1994). The channels encoded by the *eag*-related genes are relatively slowly activating, as compared with Kv class potassium channels (Ludwig et al., 1994; Sanguinetti et al., 1995; Terlau et al., 1996), and have some similarities to slowly activating potassium currents that are important in determining the threshold firing properties of neurons (Brown, 1988; Yamada et al., 1989; Wang and McKinnon, 1995). As might be anticipated from the biophysical properties of these channels, mutations in either the *eag* gene or the *erg* gene of *Drosophila* result in a hyperexcitable phenotype (Ganetzky and Wu, 1983; Titus et al., 1997; Wang et al., 1997).

The *erg* gene recently has become the center of considerable interest because mutations in this gene have been shown to underlie one form of a human genetic disease known as long QT syndrome, which gives rise to arrhythmias and an increased incidence of sudden death (Curran et al., 1995; Sanguinetti et al., 1996a). It is thought that the *erg* gene encodes the channel that underlies a previously identified potassium current known as I_{Kr} (Sanguinetti et al., 1995, 1996a; Trudeau et al., 1995). This current was described originally in cardiac myocytes (Shibasaki, 1987; Sanguinetti and Jurkiewicz, 1990), and it has been suggested that mutations in the *erg* gene may increase the susceptibility to arrhythmia, possibly by causing a prolongation of the cardiac action potential (Curran et al., 1995; Sanguinetti et al., 1996a). Alternatively, it had been suggested previously that dysfunction in the control of sympathetic outflow to the heart can induce the life-threatening arrhythmias that are characteristic of long QT syndrome (Schwartz et al., 1994).

We have shown that transcripts from the *erg* gene are expressed abundantly in the rat and human nervous systems, suggesting that the *erg* gene product might contribute to nervous system function (Wymore et al., 1997). The observation that mutations in the *erg* gene of *Drosophila* produce clear neurological defects adds further weight to this possibility (Titus et al., 1997; Wang et al., 1997). To examine further the role of the *erg* gene in the mammalian nervous system, we have conducted a systematic screen to identify genes that are related to *erg*. We have concentrated particularly on the sympathetic nervous system because of the potential clinical importance of *erg* channels in this tissue. In this paper we describe two new members of the *erg* gene family (*erg*2 and *erg*3) that are expressed exclusively in the nervous system and are expressed abundantly in sympathetic ganglia.

MATERIALS AND METHODS

Isolation of partial cDNA clones. Two sets of degenerate oligonucleotides directed against conserved regions of the *eag*, *erg*, and *elk* gene family were designed.

Set 1 was directed against the amino acid sequences "APQNTF" and "FK(AT)(ITV)WDW": forward, GC(ACGT) CC(ACGT) CA(AG) AA(CT) AC(ACGT) TT(CT); and reverse, CCA (AG)TC CCA (ACGT)(AG)(CT) (ACGT)G(CT) (CT)TT (AG)AA.

Set 2 was directed against the amino acid sequences "FK(AT)(ITV)WDW" and "HWLACIWY": forward, TT(CT) AA(AG) (AG)C(ACGT) (AG)(CT)(ACGT) TGG GA(CT) TGG; and reverse, (AG)TA CCA (AGT)AT (AG)CA (ACGT)GC (ACGT)AG CCA (AG)TG.

Using these two sets of oligonucleotides, we prepared cDNA fragments by reverse transcription and PCR amplification from total cellular RNA isolated from rat superior cervical ganglia (SCG). The amplified cDNA fragments were gel-purified and then subcloned into pBluescript SK II (Stratagene, La Jolla, CA) and analyzed by manual sequencing. Using this procedure, we identified two novel classes of *erg*-related cDNA clones. The *erg*3 cDNA initially was isolated by using the first set of oligonucleotides, and the *erg*2 cDNA was identified by using the second set.

Received Aug. 18, 1997; revised Sept. 25, 1997; accepted Sept. 26, 1997.

This work was supported by National Institutes of Health Grants NS-29755, NS-01718, HL-20558, and DK07521. We thank Dr. Michael Sanguinetti (University of Utah) for the gift of the *erg*1 (HERG) cDNA clone and Drs. Paul Adams and Michael Rosen for helpful comments on this manuscript.

Correspondence should be addressed to Dr. Jane E. Dixon, Department of Neurobiology and Behavior, State University of New York at Stony Brook, Stony Brook, NY 11794-5230.

Figure 1. Alignment of the *erg*1, *erg*2, and *erg*3 deduced amino acid sequences. There is 63% identity between *erg*2 and *erg*1, 57% identity between *erg*3 and *erg*1, and 61% identity between *erg*2 and *erg*3. Residues that are identical in all three sequences are shown with *black shading*, residues identical in two sequences are shown with *dark gray shading*, similar residues are shown with *light gray shading*, and nonconserved residues are shown *without shading*. The *erg*1 sequence corresponds to the human *erg* gene (Warmke and Ganetzky, 1994). The *erg*2 and *erg*3 sequences are from rat. The six hydrophobic domains (*S1–S6*), the pore (*P*), and the putative cyclic nucleotide binding domain (*cNBD*) are *overlined*.

Isolation of full-length ERG2 and ERG3 cDNA clones. Full-length rat *erg*2 and *erg*3 cDNA sequences were obtained first by performing a modified 5′ and 3′ rapid amplification of cDNA ends (RACE) protocol (essentially as described by Frohman, 1994), using anchor oligonucleotides complementary to the partial *erg*2 and *erg*3 clones. This required several rounds of RACE in both directions to obtain sequences with complete open reading frames. For *erg*2 the tissue source for synthesizing the cDNA used in the RACE protocol was celiac ganglia, and for *erg*3 the tissue source was brain.

Once cDNAs were obtained that extended beyond both the 3′ and 5′ ends of the open reading frame, oligonucleotides complementary to noncoding regions at either end of the coding sequence were designed, and full-length cDNA clones were obtained by using the Expand High Fidelity PCR system (Boehringer Mannheim, Indianapolis, IN) for PCR

amplification. For *erg*2, the following oligonucleotides were used to amplify full-length cDNA clones from rat celiac ganglia RNA, giving a 32 and 497 bp 5′ and 3′ untranslated region (UTR), respectively: forward, GAG TAA CTC CCA GCA AGT GC; and reverse, ACT GTT ATG AGA GTC TCA GGG G.

For *erg*3, the following oligonucleotides were used to amplify full-length cDNA clones from rat brain RNA, giving a 182 and 37 bp 5′ and 3′ UTR, respectively: forward, GAT GGA TTG GAC TTC GGC; and reverse, GCA CTT ACA TTG GAT GTG GAG.

Full-length cDNAs were subcloned into the pBluescript SK II vector. Two *erg*2 clones were sequenced in their entirety, using a combination of manual and automatic sequencing. One *erg*3 clone was sequenced in its entirety, using a combination of manual and automatic sequencing; a second independent sequence was obtained by sequencing the *erg*3 clones obtained by RACE. Differences between the two sequences were resolved by partial sequencing of a second full-length *erg*3 cDNA clone, which also was obtained from brain. Sequence alignment was performed with the Clustal W program (Thompson et al., 1994). Sequences were submitted to GenBank, with accession numbers AF016192 and AF016191 for *erg*2 and *erg*3, respectively.

Preparation of RNA. Tissue samples were quick-frozen in liquid N_2 and then homogenized in guanidinium thiocyanate. Total RNA was prepared by pelleting the homogenate over a CsCl step gradient as described previously (Dixon and McKinnon, 1996). Poly(A^+) RNA was prepared with paramagnetic poly-dT beads (Dynal, Oslo, Norway) as described previously (Wymore et al., 1997). All RNA samples were quantitated carefully by spectrophotometric analysis.

RNase protection assay. RNA probes were prepared as described previously (Dixon and McKinnon, 1994). In all cases a significant amount of nonhybridizing sequence (~50–80 bp) was included in the probe to allow for easy distinction between the probe and the specific protected band. The specificity of the assay was such that there was no evidence for unwanted cross-reaction between any probe and another nonspecific potassium channel transcript.

RNase protection assays were performed as described previously (Dixon and McKinnon, 1996). For each sample point 5 μg of total RNA or 1 μg of poly(A^+) RNA was used in the assay. A species-specific cyclophilin probe was included in the hybridization as an internal control to confirm that the sample was not lost or degraded during the assay. Five micrograms of yeast tRNA were used as a negative control to test for the presence of probe self-protection bands. RNA expression was quantitated directly from dried RNase protection gels with a PhosphorImager (Molecular Dynamics, Sunnyvale, CA).

Expression of erg *channels in* Xenopus *oocytes.* Full-length *erg*1, *erg*2, and *erg*3 cRNA transcripts were synthesized *in vitro*. The *erg*1 clone was a human cDNA that has been described previously (Sanguinetti et al., 1995) (a gift from Dr. Michael Sanguinetti, University of Utah).

Oocytes were prepared from mature female *Xenopus laevis*, using established procedures (Colman, 1984). Defolliculation was performed by incubation for 2 hr in 2 mg/ml collagenase (Type VIII, Sigma, St. Louis, MO) in Ca^{2+}-free OR2 oocyte medium with gentle agitation. Oocytes were stored in OR3 solution [50% L-15 medium (Life Technologies, Gaithersburg, MD), 1 mM glutamine, 15 mM Na-HEPES, pH 7.6, and 0.1 mg/ml gentamicin] at 18°C. Oocytes were injected with 50 nl of cRNA (~0.3 ng/nl) by using a microdispenser and a micropipette with a tip diameter of 10–20 μm. Injected oocytes were incubated at 18°C for 24–48 hr before analysis.

Oocytes were voltage-clamped with a two-microelectrode voltage clamp. Intracellular electrodes filled with 3 M KCl with resistances of 0.5–3 MΩ were used. The standard extracellular recording solution contained (in mM): 80 NaCl, 5 KCl, 1.8 $CaCl_2$, 1 $MgCl_2$, and 5 Na-HEPES, pH 7.6. Data collection and analysis were performed with pClamp software (Axon Instruments, Foster City, CA). The methanesulfonanilide E4031 was obtained from Eisai Company (Tokodai, Japan).

RESULTS

Isolation and properties of the *erg*2 and *erg*3 cDNA clones

Two partial cDNA clones, which identified two novel potassium channel genes, were isolated from rat SCG cDNA. The cDNAs were cloned by PCR, with primers that were directed against conserved regions of the *eag*, *erg*, and *elk* gene families. These partial sequences were closely related to the previously described h-*erg* (or HERG) gene (Warmke and Ganetzky, 1994), which we will refer to in the following discussions as *erg*1. Full-length *erg*2 and *erg*3 cDNA clones were obtained (see Materials and Methods for details) and sequenced in their entirety (Fig. 1). Identification of the initiator methionine and the start of the open reading frame was facilitated by the high degree of similarity in this region among the three genes. There is a short region of conservation in the three sequences at the C terminus immediately before the presumptive stop codon, which suggests that the derived amino acid sequences correctly identify the entire coding regions of all three genes.

Table 1. Amino acid identity among the *erg* family of potassium channels

	h-*erg*1	r-*erg*2	r-*erg*3	d-*erg*	m-*eag*	d-*elk*
*erg*1	100	63	57	43	31	27
*erg*2		100	61	41	32	32
*erg*3			100	44	32	25
d-*erg*				100	26	24
m-*eag*					100	29
d-*elk*						100

Multiple sequence alignment of entire deduced amino acid sequence was performed using the ClustalW program (Thompson et al., 1994). h-*erg*1 is human *erg* (Warmke and Ganetzky, 1994), r-*erg*2 and r-*erg*3 are the rat sequences reported in this paper, d-*erg* is *Drosophila erg* (Titus et al., 1997), m-*eag* is mouse *eag* (Warmke and Ganetzky, 1994), and d-*elk* is *Drosophila elk* (Warmke and Ganetzky, 1994).

At the amino acid level the three mammalian *erg* genes had identity scores of ~60% over the entire deduced amino acid sequence (Table 1). The *erg*2 sequence was 63% identical and the *erg*3 sequence was 57% identical to the *erg*1 gene, and the *erg*2 sequence was 61% identical to the *erg*3 sequence. All three mammalian *erg* sequences had similar identity scores (~42%) in comparisons with the *Drosophila erg* gene, suggesting that they all derive from a common gene. Identity with the other members of the *eag* gene family (*eag* and *elk*) was significantly lower, ~30% overall. This result suggests that the *erg*1, *erg*2, and *erg*3 genes form a distinct subfamily.

There are three highly conserved domains in the three sequences: the initial N-terminal sequence, the hydrophobic core, and the putative cyclic nucleotide binding domain. Curiously, the *Drosophila erg* sequence lacks this conserved N-terminal domain (Titus et al., 1997; Wang et al., 1997), although it is present in all three mammalian *erg* sequences as well as in the *eag* and *elk* sequences. It is known that the mammalian *erg* genes can produce alternative spliced transcripts that lack the N-terminal coding region (London et al., 1997), and it is possible that there is also alternative splicing of the *Drosophila erg* gene products and that some *Drosophila erg* mRNA species may include this domain. A short, completely conserved motif (SDPG) is found in the extreme C terminus of all three mammalian *erg* sequences.

Tissue distribution of *erg*2 and *erg*3 gene expression

The *erg*1 gene is expressed in the hearts of all species tested to date (Wymore et al., 1997) and is thought to encode one component of the delayed rectifier potassium current found in heart (Sanguinetti et al., 1995; Trudeau et al., 1995). Mutations in the *erg*1 gene have been shown to be associated with the LQT2 form of the human genetic disease long QT syndrome, which involves a significantly increased susceptibility to arrhythmias triggered by emotional or physical stress (Curran et al., 1995; Sanguinetti et al., 1996a). For this reason, we first examined *erg*2 and *erg*3

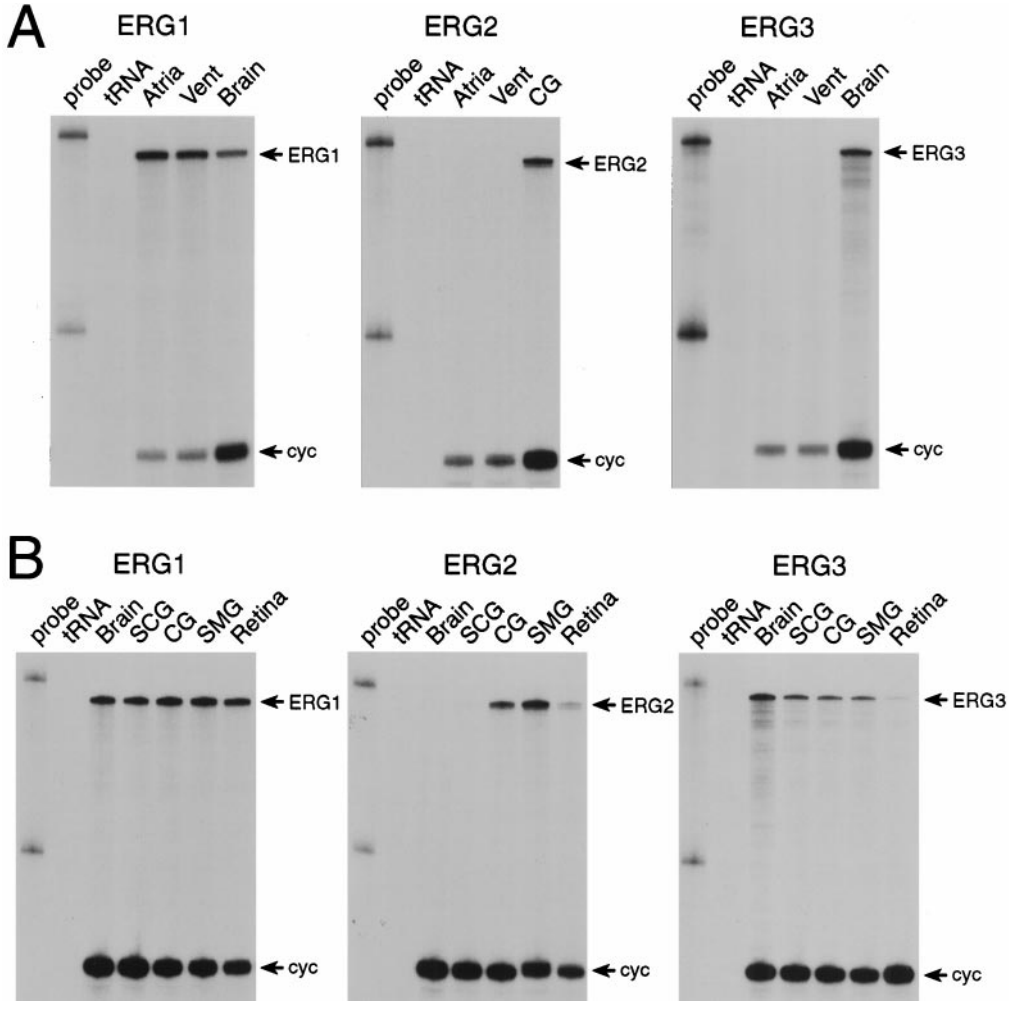

Figure 2. *erg* potassium channel mRNA expression in heart and neural tissues determined by RNase protection analysis. *A*, Neither *erg*2 nor *erg*3 mRNA is expressed at detectable levels in atrial or ventricular (*Vent*) muscle, in marked contrast to *erg*1, which is abundant in both tissues (*arrows*). The positive control samples are celiac ganglia (*CG*) or brain mRNA. *B*, All three *erg* genes are expressed in neural tissue. Samples tested were brain, superior cervical ganglia (*SCG*), celiac ganglia (*CG*), superior mesenteric ganglia (*SMG*), and retina. The cyclophilin gene (*cyc*, *arrows*) was used as an internal positive control; as has been shown previously, cyclophilin expression was always lower in muscle tissues, as compared with other tissues.

mRNA expression in heart. Neither gene is expressed at detectable levels in either atrial or ventricular muscle, in marked contrast to the results obtained with the *erg*1 gene (Fig. 2*A*).

As shown previously (Wymore et al., 1997), the *erg*1 gene is expressed abundantly in brain and in retina. Intriguingly, given the clinical symptoms associated with mutations in the *erg*1 gene, *erg*1 mRNA is expressed abundantly in sympathetic ganglia (Fig. 2*B*). This result suggests that mutations in the *erg*1 gene could affect sympathetic regulation of cardiac function in addition to having direct effects on myocardial function.

The *erg*2 gene has a very restricted distribution in neural tissues and is not expressed at detectable levels in brain. Although initially cloned by PCR amplification from SCG mRNA, *erg*2 expression in SCG is also very low. The peripheral sympathetic nervous system has two anatomically and functionally distinct components: the paravertebral ganglia and the prevertebral ganglia. It has been shown previously that the electrophysiological properties of neurons in the paravertebral ganglia, such as the SCG, are very uniform, whereas there are at least two electrophysiologically distinct types of neurons in the prevertebral ganglia (Cassell et al., 1986; Wang and McKinnon, 1995, 1996). The molecular basis for this differentiation currently is undetermined (Dixon and McKinnon, 1996). The *erg*2 gene is expressed abundantly in the two prevertebral sympathetic ganglia examined: the celiac ganglia (CG) and the superior mesenteric ganglia (SMG) (Fig. 2*B*). This result suggests that the *erg*2 channel could contribute to the electrophysiological differentiation of prevertebral neurons, but identification of the native current corresponding to the *erg*2 channel is necessary before this conclusion can be established. There is also a low level of *erg*2 expression in retina.

The *erg*3 gene is broadly expressed throughout the nervous system, similar to *erg*1. In addition to brain, *erg*3 mRNA is expressed in all of the sympathetic ganglia tested and also is expressed at low levels in retina (Fig. 2*B*).

Expression of all three *erg* genes in sympathetic ganglia prompted us to examine expression in PC12 cells, a cell line that often is used as a cell culture analog of sympathetic neurons. Both the *erg*1 and *erg*2 genes are expressed in PC12 cells, whereas the *erg*3 gene is not expressed (Fig. 3*A*). A further elaboration of the neuronal phenotype of PC12 cells can be induced by treatment with nerve growth factor (NGF). Exposure to NGF resulted in little change in *erg*1 mRNA expression in PC12 cells. In contrast,

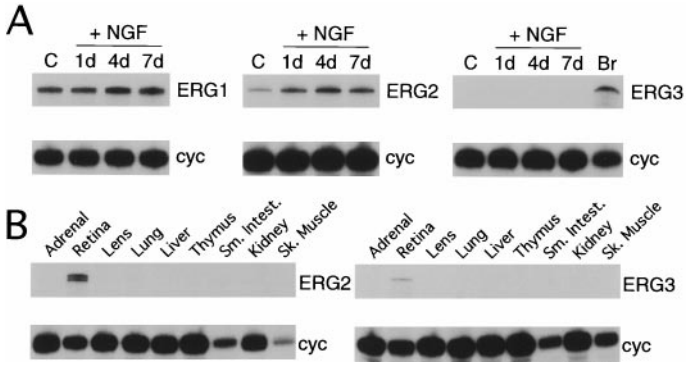

Figure 3. *erg* potassium channel mRNA expression in PC12 cells and non-neural tissues determined by RNase protection analysis. *A*, *erg* mRNA expression in PC12 cells in control media or after 1, 4, or 7 d of treatment with nerve growth factor (*NGF*). Brain (*Br*) mRNA was used as a positive control for the *erg*3 experiment. *B*, Expression of *erg*2 and *erg*3 mRNA in non-neural tissues. Retinal RNA was used as the positive control.

upregulation of *erg*2 mRNA was marked and relatively rapid (~threefold after 1 d). No induction of *erg*3 gene expression was observed after NGF treatment.

Neither the *erg*2 nor the *erg*3 gene was expressed in any of the non-neural tissues that were tested (Fig. 3*B*), suggesting that expression of these genes is nervous system-specific. This is in marked contrast to the *erg*1 gene, which is expressed in several non-neuronal tissues, including adrenal gland, thymus, and lung (Wymore et al., 1997).

Kinetic properties of the *erg*2 and *erg*3 potassium channels

The kinetic properties of the *erg*1, *erg*2, and *erg*3 channels were compared by expressing the channels in *Xenopus* oocytes. The waveform of the current elicited in response to a depolarizing voltage step to +20 mV was markedly different for the *erg*3 channel as compared with the other two channels (Fig. 4). The *erg*1 and *erg*2 channels were relatively slowly activating delayed rectifiers, whereas the *erg*3 current had a predominant transient component that decayed to a sustained plateau. The kinetic properties of the *erg*1 channel were very similar to those described previously (Sanguinetti et al., 1995; Spector et al., 1996).

The kinetic basis for the different waveforms was determined by examining the activation and inactivation kinetics of the three channels. The *erg*3 channel activated at significantly faster rates than did either the *erg*1 or *erg*2 channels over the entire voltage range tested (Fig. 5: note that the time scale for the *erg*3 records is fivefold faster than for the other two channels). The *erg*1 channel had generally faster activation rates than did the *erg*2 channel. Over the time course studied, activation of the *erg*1 channel was approximated reasonably well by a single exponential. Activation of the *erg*2 channel clearly required two exponentials, with the faster component becoming predominant at more positive potentials. Activation of the *erg*3 channel was clearly sigmoidal at negative potentials. The transient component of the *erg*3 current became prominent at step potentials positive to −10 mV. All three channels display a characteristic reduction in steady-state current at positive potentials, producing a negative slope *I–V* relationship. The large size of the tail currents relative to the currents elicited by the depolarizing voltage steps is attributable to the rapid relief of steady-state inactivation after the step back to −70 mV (see Fig. 7*B*).

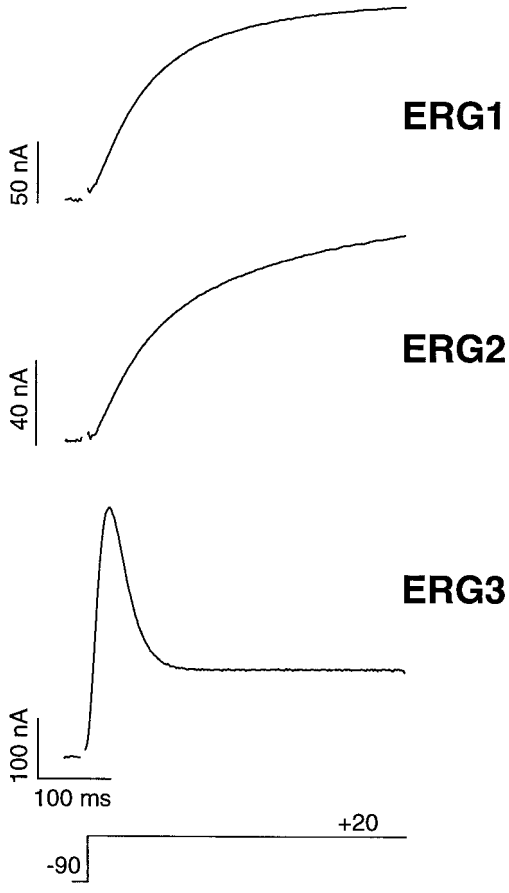

Figure 4. Current responses of the *erg*1, *erg*2, and *erg*3 channels to a depolarizing voltage step. The holding potential was −90 mV, and the step was to +20 mV. Recordings were from *Xenopus* oocytes and were performed with two-electrode voltage clamp. Current records were leakage-subtracted, and the capacitance artifact at the beginning of the voltage step was blanked.

The *erg*1 channel and the corresponding native I_{Kr} current are known to have very unusual inactivation kinetics, with the inactivation rate being significantly faster than the activation rate at most membrane potentials (Shibasaki, 1987; Smith et al., 1996; Spector et al., 1996). For this reason, we compared the inactivation rates of the three channels, using the triple pulse protocol described previously for *erg*1 (Smith et al., 1996; Spector et al., 1996). The inactivation process could be well described by a single exponential for all three channels. Inactivation of the *erg*1 and *erg*2 channels had virtually identical time courses over the entire range of potentials tested (Fig. 6). In marked contrast, the *erg*3 channel inactivated significantly more slowly at membrane potentials positive to −40 mV.

It can be seen from these data that the appearance of a transient waveform at positive potentials in the *erg*3 currents, but not the *erg*1 and *erg*2 currents, is attributable to differences in the relative rates of activation and inactivation. The ratio between the inactivation and activation rates of the *erg*3 channel was close to two at positive potentials, whereas inactivation rates were at least 10-fold faster than activation rates for both the *erg*1 and *erg*2 channels in this potential range. For the *erg*1 and *erg*2 channels, the inactivation process is in quasi-steady-state relative to the much slower activation process. The transient waveform of the *erg*3 current is produced by much the same mechanism as for a

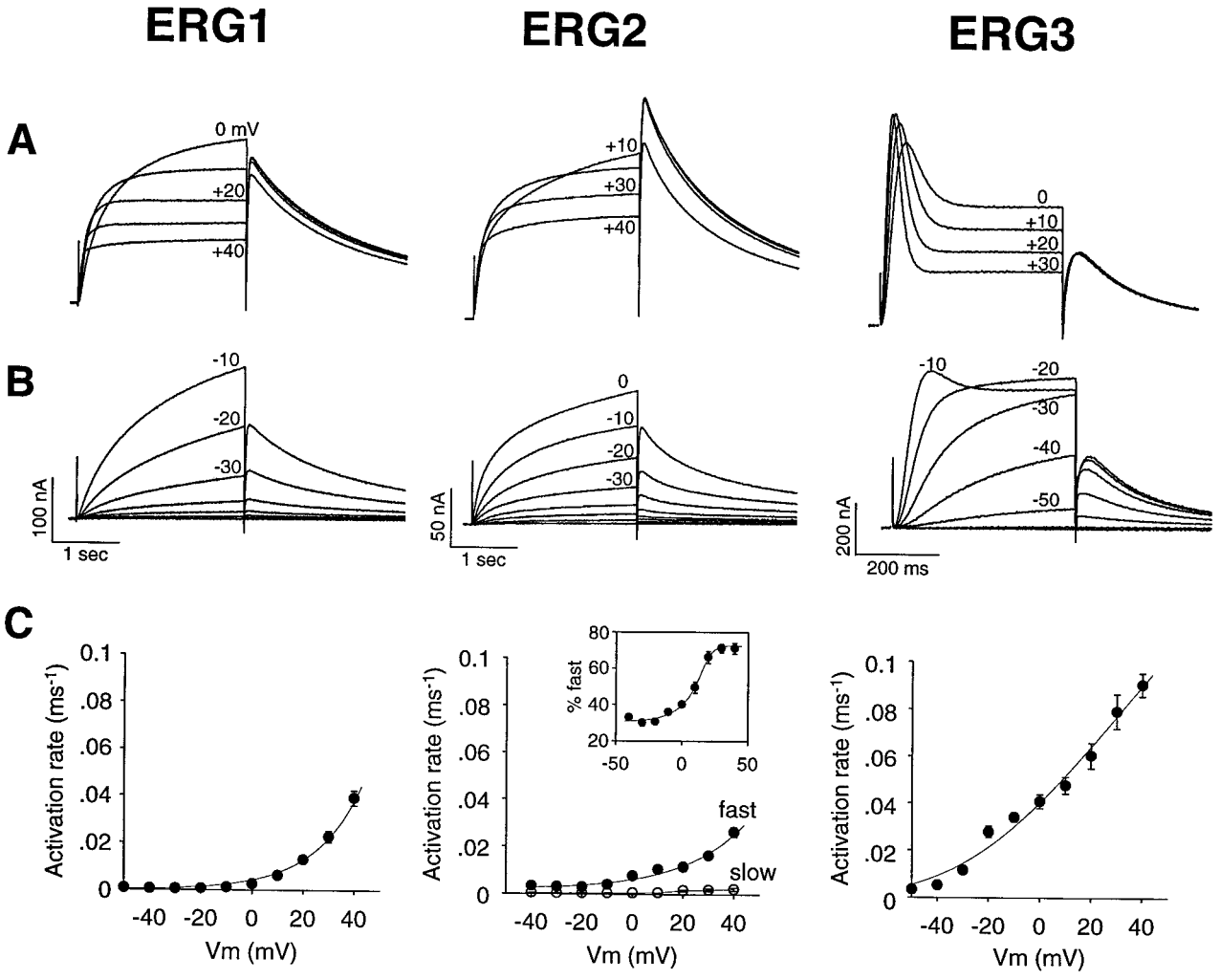

Figure 5. Activation rates of the *erg*1, *erg*2, and *erg*3 channels. *A*, *B*, Current traces showing channel activation and deactivation in response to voltage steps to various potentials from a holding potential of −90 mV. Tail currents were recorded at −70 mV. Note the much faster time scale for *erg*3 as compared with the *erg*1 and *erg*2 channels. Current records were leakage-subtracted. *C*, Comparison of the activation rates of the *erg*1, *erg*2, and *erg*3 channels. Activation rates were measured as the inverse of the time constant of single or double exponentials fit to the current traces. A single exponential gave a good fit for *erg*1. For *erg*2, two exponentials were required, and the fraction of the fast component is shown in the *inset*. For *erg*3, activation was clearly sigmoidal at negative potentials. In these cases the activation time course was fit with a single exponential after a delay, to allow for direct comparison with the other two channels. Data are averages from seven or eight cells; error bars are SEM.

typical "A current," which has an inactivation rate that is similar or somewhat slower than the activation rate. The primary difference between the *erg*3 current and a typical A current is the persistence of a maintained plateau current, which is attributable to the very shallow steady-state inactivation curve of the *erg*3 channel.

There were other differences among the three *erg* channels that are of potential relevance to the physiological function of these channels. The peak conductance–voltage relationship was significantly different for each of the three channels (Fig. 7*A*). The midpoint for activation shifted ~20 mV among the three channels, from −44 ± 1.4 mV for *erg*3 to −20 ± 1.0 mV for *erg*1 to −3.5 ± 0.6 mV for *erg*2 (n = 7 or 8). The *erg*1 and *erg*2 channels had generally similar steady-state inactivation, or rectification properties, whereas the slope of the rectification curve for the *erg*3 channel was significantly shallower, although the midpoint was similar to the other channels (Fig. 7*B*). This difference in slope meant that the *erg*3 channel had less steady-state inactivation at potentials positive to −100 mV than did the other two channels.

The physiological function of the *erg* channels in the nervous system is currently obscure, although the *Drosophila erg* channel clearly acts to reduce neuronal excitability (Titus et al., 1997; Wang et al., 1997). We examined the potential contribution of the *erg* channels to the steady-state current around the threshold for spike initiation (approximately −35 mV) in two independent ways. Initially, the fraction of channels activated at each potential (Fig. 7*A*) was multiplied by the fraction of channels inactivated at that potential (Fig. 7*B*) to give the fraction of channels open at steady-state (Fig. 7*C*). A second, more direct approach was to measure the conductance at the end of a sustained voltage step; then, to normalize for differences in expression between different oocytes and channels, the conductance at each potential was divided by the maximum conductance to give a normalized steady-state conductance (Fig. 7*D*). There was good agreement between the two methods used for calculating the shape and relative peaks of the steady-state conductance (compare Fig. 7, *C* and *D*).

The steady-state conductance or "window current" was large

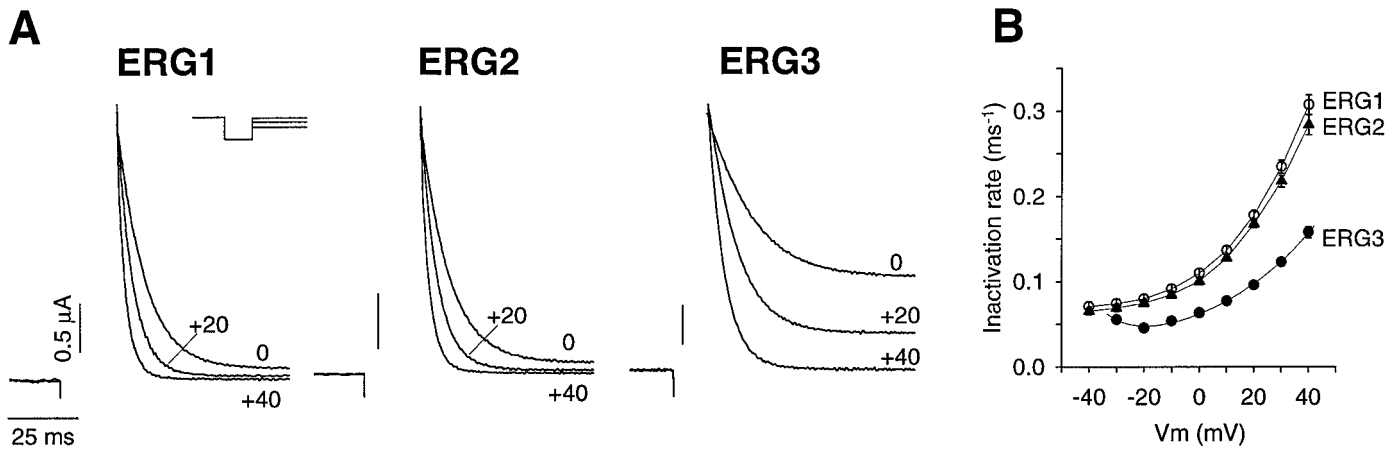

Figure 6. Inactivation rates of the *erg*1, *erg*2, and *erg*3 channels. *A*, Current traces showing channel inactivation at 0, +20, and +40 mV. Membrane potential was depolarized to +40 mV for 1000 msec to activate the channels fully. For *erg*1 and *erg*2, a brief (15–20 msec) hyperpolarizing step to −95 mV was used to allow for recovery from inactivation before the depolarizing voltage step shown in the recordings. For *erg*3, because the rate of deactivation was significantly faster than for the other two channels, a slightly modified protocol was used. The hyperpolarizing step was shorter (7 msec), and the step potential was more positive (−70 mV). With the use of this protocol minimal deactivation (<6%) occurred so that during the subsequent depolarization step the kinetics of inactivation were not significantly contaminated by reactivation. *B*, Comparison of the inactivation rates of the *erg*1, *erg*2, and *erg*3 channels. Inactivation rates were measured as the inverse of the time constant of a single exponential fit to the current traces. Data are averages from seven cells; error bars are SEM.

for the *erg*3 channel, whereas the *erg*1 and *erg*2 channels passed significantly less current. Below −35 mV, the region important for control of spike initiation, the difference was even more striking, with the steady-state *erg*3 conductance close to a maximum and the *erg*1 and *erg*2 conductances at relatively low values.

Pharmacological properties of the *erg*2 and *erg*3 potassium channels

A characteristic pharmacological property of the I_{Kr} current, which is thought to be encoded by the *erg*1 gene, is its sensitivity to methanesulfonanilides (Sanguinetti and Jurkiewicz, 1990). The sensitivity of all three channels to blockade by the methanesulfonanilide E4031 was determined (Fig. 8). The K_D for blockade by E4031 was similar for all three channels (99, 116, and 193 nM for *erg*1, *erg*2, and *erg*3, respectively), which is consistent with the high degree of conservation in the pore region of these channels. As has been described previously for the blockade of the *erg*1 channel by other methanesulfonanilide drugs (Snyders and Chaudhary, 1996; Spector et al., 1996), E4031 acted as an open channel blocker. The on-rate for binding was apparently very slow, and repeated depolarizing pulses were required to reach quasi-steady-state for drug binding, particularly at low drug concentrations.

DISCUSSION

In this paper we describe the identification, mRNA distribution, and biophysical properties of two new members of the *erg* potassium channel gene family: *erg*2 and *erg*3. Both genes are expressed exclusively in neural tissue, in marked contrast to the previously described *erg*1 gene, which is expressed in a wide range of tissues in addition to the nervous system (Wymore et al., 1997). The *erg*3 gene is expressed abundantly in brain and sympathetic ganglia. Distribution of *erg*2 gene expression is restricted considerably more and is located primarily in a subset of sympathetic ganglia known as the prevertebral ganglia.

The physiological role of the *erg* channels in the mammalian nervous system is currently uncertain. In *Drosophila* it has been shown that mutations in the *erg* gene produce a hyperexcitable phenotype (Titus et al., 1997; Wang et al., 1997), suggesting that the *erg* channel inhibits neuronal excitability. The biophysical properties of the *Drosophila erg* channel have yet to be characterized, however, and the native current produced by the *erg* channels has not been described. A current with pharmacological and kinetic properties that are very similar to those of *erg* channels has been described in a rat dorsal root ganglia cell line (Farvelli et al., 1996). Pharmacological blockade of this current results in a significant decrease in spike frequency adaptation and an increase in excitability in response to maintained depolarizing stimuli (Chiesa et al., 1997), suggesting that *erg* channels can contribute to the control of neuronal excitability in some mammalian cells. The observation that all three *erg* channels are very sensitive to blockade by methanesulfonanilides such as E4031 should make it possible to determine the function of the *erg* channels in the nervous system, although the relatively slow onset and voltage dependence of binding means that some caution will be required in interpreting negative results.

Several differences in the functional properties of the three *erg* channels were found that could be of physiological importance. Most obvious was the difference in the waveform of the currents produced in response to voltage steps to positive membrane potentials. The current produced by the *erg*3 channel had a large transient component at positive potentials, whereas the other two channels produced slowly activating currents that resembled classical delayed rectifiers. The kinetic basis for the switch between the two waveforms was somewhat paradoxical. For the *erg*1 and *erg*2 channels, the delayed rectifier waveform was produced by an *increase* in the inactivation rate relative to the inactivation rate of the *erg*3 channel. This result is attributable to the very unusual kinetic properties of the *erg*1 and *erg*2 channels, which have significantly faster inactivation than activation rates (typically at least 10-fold faster). The activation rate was significantly slower for the *erg*1 and *erg*2 channels than for the *erg*3 channel, and this difference also contributed to the production of different waveforms.

A more subtle difference, which is of potential importance for the physiology of the cells that express *erg* channels, was the

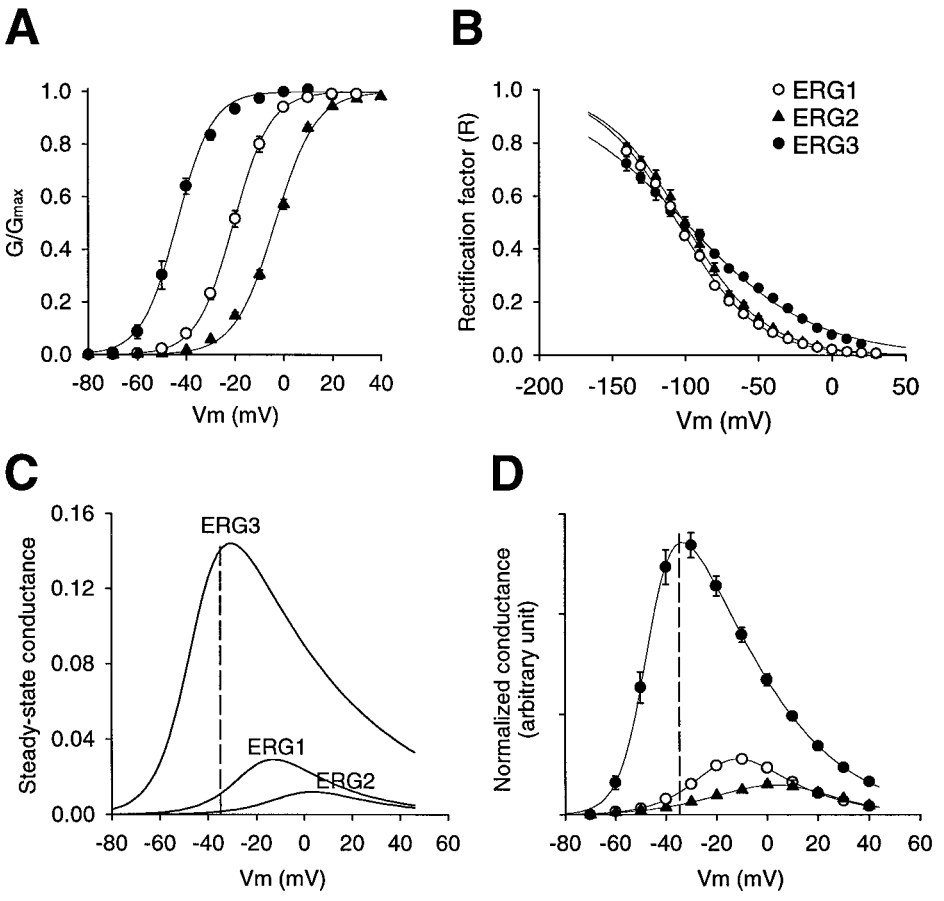

Figure 7. Steady-state kinetic properties of the *erg*1, *erg*2, and *erg*3 channels. *A*, Peak conductance–voltage curves were measured by stepping to the test potential from a holding potential of −90 mV, followed by a step back to the holding potential. The sizes of the tail currents after recovery from inactivation were used as a measure of channel activation during the test step. The step duration was 5 sec for *erg*1 and *erg*2 and 1 sec for *erg*3. Data points are the average of seven or eight cells and were fit with the Boltzmann equation: $G/G_{max} = 1/(1 + \exp((V - V_h)/k_h))$, where $V_h = -21 \pm 1.0$, -3.5 ± 0.6, and -44 ± 1.4 mV and $k_h = -7.6 \pm 0.4$, -8.3 ± 0.3, and -7.2 ± 0.2 mV for *erg*1, *erg*2, and *erg*3, respectively. The *open circle* represents *erg*1, the *filled triangle* represents *erg*2, and the *filled circle* represents *erg*3. *B*, Rectification factor or steady-state inactivation curve. This was measured by using a protocol similar to that described previously (Sanguinetti et al., 1995). Channels were fully activated by stepping to +40 mV for 1 sec. Then the fully activated *I–V* relationship was determined by stepping back to various test potentials. Tail currents were extrapolated back to $t = 0$ to correct for deactivation where necessary. Slope conductance was determined from the *I–V* plot between −140 and −120 mV, and then the rectification factor was calculated with the following formula: $R = I/(G_{slope}(V_m - E_K))$, where *R* is the rectification factor. Data points are the average of three or four cells and were fit with the Boltzmann equation. $V_h = -101 \pm 2.4$, -105 ± 0.3, and -100 ± 3.0 mV and $k_h = 28 \pm 0.7$, 27 ± 0.2, and 43 ± 1.2 mV for *erg*1, *erg*2, and *erg*3, respectively. *C*, Calculated steady-state conductance–voltage curve. This was calculated by multiplying the fit conductance–voltage and rectification factor curves together for each channel. The *dashed line* corresponds to $V_m = -35$ mV, which is the threshold for spike initiation in a typical sympathetic neuron. *D*, Normalized steady-state conductance–voltage curve. This was measured by calculating the steady-state conductance–voltage curve and then normalizing to the tail current at −90 mV after complete activation of the current by a step to +40 mV. The tail current was extrapolated back to $t = 0$ to correct for deactivation. This procedure normalized for different levels of expression between different oocytes and different channels. Although this procedure did not give absolute values for the fractional conductance, it did allow direct comparison of the relative heights and shapes of the *G–V* curve for the three channels. Symbols have the same representations as in *A* and *B*. Data points are averages from six or eight cells; error bars are SEM.

difference in the position and peak of the steady-state conductance–voltage curve of the three channels. The *erg*3 channel activated at relatively negative membrane potentials and produced a large window current, which peaked around the threshold for spike initiation in a typical sympathetic neuron (Wang and McKinnon, 1995). The *erg*3 channels could, therefore, produce a significant inhibitory influence on subthreshold electrical excitability. The conductance–voltage curve for the *erg*1 and *erg*2 channels was shifted to the right, and the peak steady-state conductance was significantly lower relative to the *erg*3 channel. This makes it less likely that these channels could influence the threshold firing properties of neurons, at least as homomultimers. In cardiac myocytes the action potential duration is relatively long, giving the *erg*1 channels sufficient time to activate fully and contribute to action potential repolarization. The relatively brief duration of the typical neuronal action potential means that there would be relatively little activation of the *erg*1 or *erg*2 channels during a single action potential. It is possible that the very slow deactivation kinetics of these channels could result in cumulative activation of the channels during a prolonged burst of action potentials. Even in this case, however, the relatively positive activation threshold of these channels would limit their influence on neuronal excitability. It is possible, or even likely, that the functional properties of the *erg*1 and *erg*2 channels are modified by heteromultimer formation. The broad expression of the *erg*3 channel in the nervous system makes it an obvious candidate, but other, yet to be identified, subunits also could modify the kinetic properties of the channels significantly, as has been shown recently for the KvLQT1 channel (Barhanin et al., 1996; Sanguinetti et al., 1996b).

The discovery that in mammals there is a small family of *erg* genes may have implications for the etiology of one form of the human genetic disease known as long QT syndrome (LQT). It has been shown that three forms of the autosomal dominant LQT syndrome (Romano–Ward syndrome) are produced by mutations in ion channel genes expressed in the heart. LQT1 syndrome involves mutations in the KvLQT1 gene, which encodes a slowly activating K^+ channel that probably underlies I_{Ks} in cardiac myocytes (Barhanin et al., 1996; Sanguinetti et al., 1996b). LQT2 syndrome involves mutations in the *erg*1 (or HERG) gene, which encodes the I_{Kr} channel (Sanguinetti et al., 1995; Trudeau et al., 1995), and LQT3 syndrome involves mutations in the cardiac sodium channel gene SCN5 (or hH1) (Wang et al., 1995). Autosomal dominant LQT syndrome characteristically displays no overt neurological symptoms (Schwartz et al., 1994). For the KvLQT1 and SCN5 genes this can be explained by the fact that these two genes are not expressed in the nervous system (Gellens et al., 1992; Wang et al., 1996). For LQT2, however, the situation

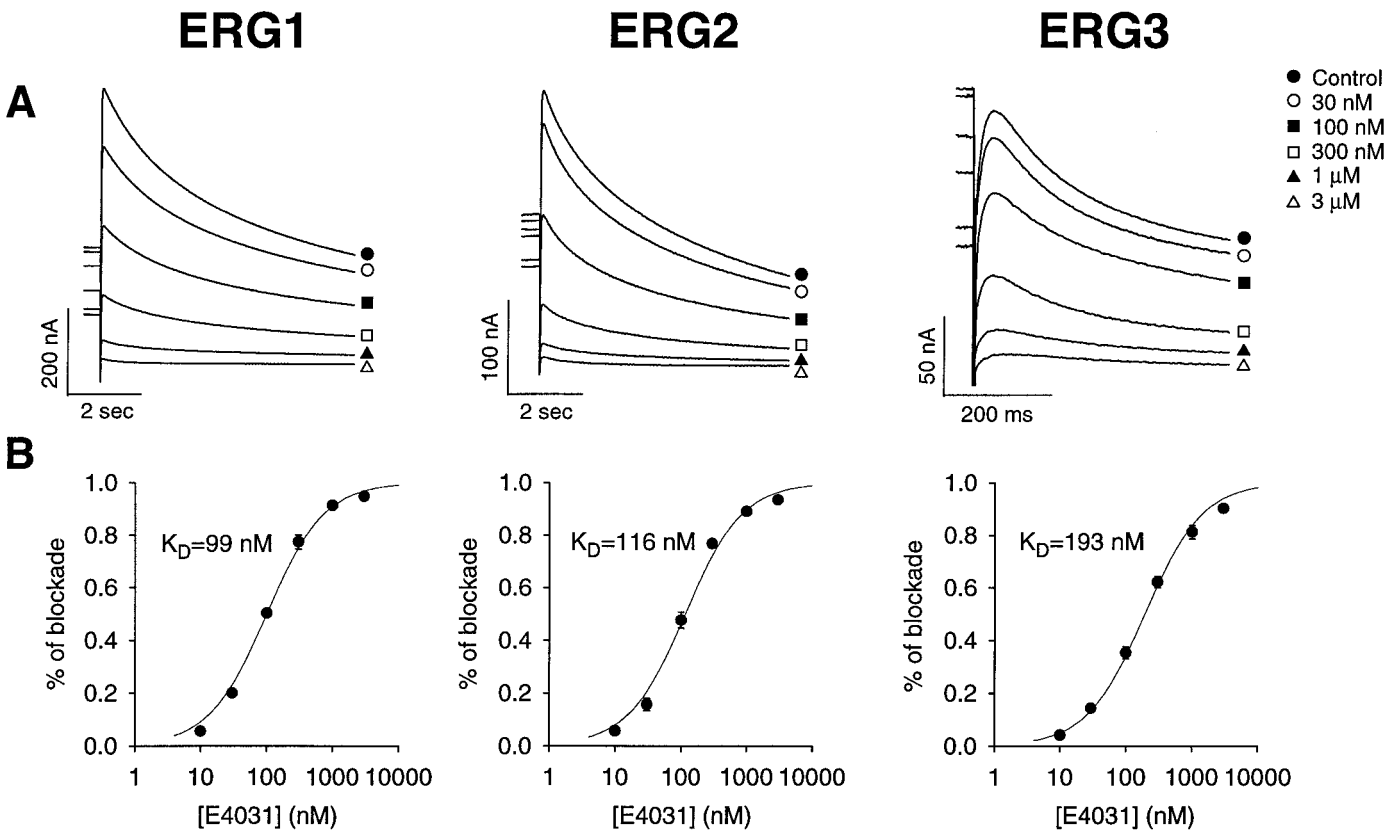

Figure 8. Inhibition of the *erg*1, *erg*2, and *erg*3 channels by the methanesulfonanilide E4031. *A*, Tail currents in the presence of increasing concentrations of E4031. The procedure used to measure the degree of blockade at each drug concentration was similar to that described previously (Snyders and Chaudhary, 1996). Because the drug is an open channel blocker with a very slow on-rate of binding, it was necessary to depolarize the cell repetitively to reach equilibrium binding. A 20 sec step to +20 mV was applied at 0.033 Hz until no further reduction in current was seen for that particular drug concentration. At that point a test step to +10 mV for 1 sec was applied, and the tail current at −60 mV was measured. *B*, Hill plots of E4031 inhibition of the *erg*1, *erg*2, and *erg*3 channels showing the K_D for channel blockade. Data points were fit with the Hill equation: percentage of blockade = $1/(1 + (K_D/[E4031]))$, where K_D = 99 ± 10, 116 ± 11, and 193 ± 18 nM for *erg*1, *erg*2, and *erg*3, respectively. Data points are averages from three or four cells; error bars are SEM.

is more complex, because the *erg*1 gene is expressed widely in the nervous system (Wymore et al., 1997). Given this distribution pattern, the apparent lack of neurological symptoms in LQT2 patients is somewhat surprising. Identification of the *erg2* and *erg*3 genes provides a potential explanation for this paradox. The cardiac-specific nature of LQT2 syndrome may be explained by the fact that the *erg*1 gene is the only member of the *erg* gene family expressed in heart, and, for this reason, cardiac function may be unusually dependent on the presence of functional *erg*1 channels. In contrast, in neural tissues, two other *erg* genes are expressed. Although the channels encoded by these genes are not identical in function to the *erg*1 channel, they are sufficiently similar to suggest that they could compensate for the reduction in functional *erg*1 channels.

The observation that the *erg*1 gene is expressed in sympathetic ganglia does, however, raise an interesting question regarding the genesis of the LQT2 form of LQT syndrome. There have been two hypotheses proposed to account for the underlying etiology of LQT syndrome (Schwartz et al., 1994; Roden et al., 1996). One hypothesis relies on the observation that the life-threatening arrhythmias characteristic of this disease are induced by increased sympathetic outflow stimulated by intense emotional or physical stress. This hypothesis has received support from the finding that the arrhythmias, syncope, and sudden death that are characteristic of the disease can be prevented in large part by β-blockade and/or cardiac sympathetic denervation. The most specific form of this hypothesis invoked a sympathetic imbalance, positing that there was excessive left sympathetic outflow to the heart (Schwartz et al., 1994). The second hypothesis holds that the defect is intrinsic to the heart, affecting the intrinsic electrophysiological function of cardiac myocytes. In the case of LQT1 and LQT3 the intrinsic defect hypothesis is likely to be a sufficient explanation for the syndrome, because the genes underlying these two forms of the disease are not expressed in the nervous system. For LQT2, however, because the *erg*1 gene is expressed abundantly in sympathetic ganglia and adrenal glands in addition to heart, the situation is more complex. Because *erg* channels can contribute to the control of neuronal excitability (Chiesa et al., 1997; Titus et al., 1997; Wang et al., 1997), disruption of *erg*1 gene function conceivably could result in hyperexcitability in sympathetic neurons, thereby affecting sympathetic outflow to the heart, particularly during periods of physiological stress. Alternatively, the adrenal glands might be unusually dependent on normal *erg*1 channel function because, like the heart, they express *erg*1, but not the other two *erg* genes. Mutations in the *erg*1 gene could result in an increase in circulating catecholamines, at least under some physiological conditions. Either of these effects potentially could contribute to the initiation of arrhythmias in LQT2 syndrome.

These possibilities are not exclusive of an intrinsic cardiac myocyte defect in LQT2 and might act synergistically with such a defect. Although the balance of evidence currently favors the intrinsic hypothesis for LQT2 syndrome, it will be of considerable importance to determine the function of the *erg* channels in the sympathetic/adrenal system to gain further insight into the etiology of the LQT2 form of long QT syndrome.

REFERENCES

Barhanin J, Lesage F, Guillemare E, Fink M, Lazdunski M, Romey G (1996) K_VLQT1 and IsK (minK) proteins associate to form the I_{Ks} cardiac potassium current. Nature 384:78–80.

Brown DA (1988) M currents. In: Ion channels (Narahashi T, ed), pp 55–94. New York: Plenum.

Cassell JF, Clark AL, McLachlan EM (1986) Characteristics of phasic and tonic sympathetic ganglion cells of the guinea-pig. J Physiol (Lond) 372:457–483.

Chiesa N, Rosati B, Arcangeli A, Olivotto M, Wanke E (1997) A novel role for HERG K^+ channels: spike frequency adaptation. J Physiol (Lond) 501:313–318.

Colman A (1984) Translation of eukaryotic messenger RNA in *Xenopus* oocytes. In: Transcription and translation (Hames BD, Higgins SJ, eds), pp 271–302. Oxford: IRL.

Curran ME, Splawski I, Timothy KW, Vincent GM, Green ED, Keating MT (1995) A molecular basis for cardiac arrhythmia: HERG mutations cause long QT syndrome. Cell 80:795–803.

Dixon JE, McKinnon D (1994) Quantitative analysis of potassium channel mRNA expression in atrial and ventricular muscle of rats. Circ Res 75:252–260.

Dixon JE, McKinnon D (1996) Potassium channel mRNA and protein expression in prevertebral and paravertebral sympathetic neurons. Eur J Neurosci 8:183–191.

Farvelli L, Arcangeli A, Olivotto M, Wanke E (1996) A HERG-like K^+ channel in rat F-11 DRG cell line: pharmacological identification and biophysical characterization. J Physiol (Lond) 496:13–23.

Frohman MA (1994) On beyond classic RACE (rapid amplification of cDNA ends). PCR Methods Appl 4:S40–S58.

Ganetzky B, Wu CF (1983) Neurogenetic analysis of potassium currents in *Drosophila*: synergistic effects on neuromuscular transmission in double mutants. J Neurogenet 1:17–28.

Gellens ME, George AL, Chen LQ, Chahine M, Horn R, Barchi RL, Kallen RG (1992) Primary structure and functional expression of the human cardiac tetrodotoxin-insensitive voltage-dependent sodium channel. Proc Natl Acad Sci USA 89:554–558.

London B, Beyer AK, Newton KP, Trudeau MC, Robertson GA (1997) Cloning a cardiac-specific isoform of HERG from the mouse. Biophys J 72:A224.

Ludwig J, Terlau H, Wunder F, Bruggemann A, Pardo LA, Marquardt A, Stuhmer W, Pongs O (1994) Functional expression of a rat homologue of the voltage-gated *ether a go-go* potassium channel reveals differences in selectivity and activation kinetics between the *Drosophila* channel and its mammalian counterpart. EMBO J 13:4451–4458.

Roden DM, Lazzara R, Rosen D, Schwartz PJ, Towbin J, Vincent GM (1996) Multiple mechanisms in the long-QT syndrome. Circulation 94:1996–2012.

Sanguinetti MC, Jurkiewicz NK (1990) Two components of cardiac delayed rectifier K^+ current: differential sensitivity to block by class III antiarrhythmic agents. J Gen Physiol 96:195–215.

Sanguinetti MC, Jiang C, Curran ME, Keating MT (1995) A mechanistic link between an inherited and an acquired cardiac arrhythmia: *HERG* encodes the I_{Kr} potassium channel. Cell 81:299–301.

Sanguinetti MC, Curran ME, Spector PS, Keating MT (1996a) Spectrum of HERG K^+-channel dysfunction in an inherited cardiac arrhythmia. Proc Natl Acad Sci USA 93:2208–2212.

Sanguinetti MC, Curran ME, Zou A, Shen J, Spector PS, Atkinson DL, Keating MT (1996b) Coassembly of K_VLQT1 and minK (IsK) proteins to form cardiac I_{Ks} potassium channel. Nature 384:80–83.

Schwartz PJ, Locati EH, Napolitano C, Priori SG (1994) The long QT syndrome. In: Cardiac electrophysiology: from cell to bedside, 2nd Ed (Zipes DP, Jalife J, eds), pp 788–811. Philadelphia: Saunders.

Shibasaki T (1987) Conductance and kinetics of delayed rectifier potassium channels in nodal cells of the rabbit heart. J Physiol (Lond) 387:227–250.

Smith PL, Baukrowitz T, Yellen G (1996) The inward rectification of the HERG cardiac potassium channel. Nature 379:833–836.

Snyders DJ, Chaudhary A (1996) High affinity open channel block by dofetilide of *HERG* expressed in a human cell line. Mol Pharmacol 49:949–955.

Spector PS, Curran ME, Keating MT, Sanguinetti MC (1996) Class III antiarrhythmic drugs block HERG, a human cardiac delayed rectifier K^+ channel. Circ Res 78:499–503.

Terlau H, Ludwig J, Steffan R, Pongs O, Stuhmer W, Heinemann SH (1996) Extracellular Mg^{2+} regulates activation of rat *eag* potassium channel. Pflügers Arch 432:301–312.

Thompson JD, Higgins DG, Gibson TJ (1994) CLUSTAL W: improving the sensitivity of progressive multiple sequence alignment through sequence weighting, position specific gap penalties, and weight matrix choice. Nucleic Acids Res 22:4673–4680.

Titus SA, Warmke JW, Ganetzky B (1997) The *Drosophila erg* K^+ channel polypeptide is encoded by the seizure locus. J Neurosci 17:875–881.

Trudeau MC, Warmke JW, Ganetzky B, Robertson GA (1995) HERG, a human inward rectifier in the voltage-gated potassium channel family. Science 269:92–95.

Wang HS, McKinnon D (1995) Potassium channel expression in prevertebral and paravertebral sympathetic neurones: control of firing properties. J Physiol (Lond) 485:319–335.

Wang HS, McKinnon D (1996) Modulation of inward rectifier currents in rat sympathetic neurones by muscarinic receptors. J Physiol (Lond) 492:467–478.

Wang Q, Shen J, Splawski I, Atkinson D, Li Z, Robinson JL, Moss AJ, Towbin JA, Keating MT (1995) SCN5A mutations associated with an inherited cardiac arrhythmia, long QT syndrome. Cell 80:805–811.

Wang Q, Curran ME, Splawski I, Burn TC, Millholland JM, VanRaay TJ, Shen J, Timothy KW, Vincent GM, de Jager T, Schwartz PJ, Towbin JA, Moss AJ, Atkinson DL, Landes GM, Connors TD, Keating MT (1996) Positional cloning of a novel potassium channel gene: *KVLQT1* mutations cause cardiac arrhythmias. Nat Genet 12:17–23.

Wang X, Reynolds ER, Deak P, Hall LM (1997) The *seizure* locus encodes the *Drosophila* homolog of the HERG potassium channel. J Neurosci 17:882–890.

Warmke J, Ganetzky B (1994) A family of potassium channel genes related to *eag* in *Drosophila* and mammals. Proc Natl Acad Sci USA 91:3438–3442.

Warmke J, Drysdale R, Ganetzky B (1991) A distinct potassium channel polypeptide encoded by the *Drosophila eag* locus. Science 252:1560–1562.

Wymore R, Gintant GA, Wymore RT, Dixon JE, McKinnon D, Cohen IS (1997) Tissue and species distribution of mRNA for the I_{Kr}-like K^+ channel, *erg*. Circ Res 80:261–268.

Yamada WM, Koch C, Adams PR (1989) Multiple channels and calcium dynamics. In: Methods in neuronal modeling (Koch C, Segev I, eds), pp 97–133. Cambridge, MA: Bradford.